Computational Study of Copper(II) Complexation and Hydrolysis in Aqueous Solutions Using Mixed Cluster/Continuum Models

Vyacheslav S. Bryantsev,* Mamadou S. Diallo, and William A. Goddard III*

Materials and Process Simulation Center, Beckman Institute 139-74, California Institute of Technology, Pasadena, California 91125

Received: May 22, 2009; Revised Manuscript Received: July 20, 2009

We use density functional theory (B3LYP) and the COSMO continuum solvent model to characterize the structure and stability of the hydrated Cu(II) complexes $[Cu(MeNH_2)(H_2O)_{n-1}]^{2+}$ and $[Cu(OH)_x(H_2O)_{n-x}]^{2-x}$ ($x = 1-3$) as a function of metal coordination number (4−6) and cluster size ($n = 4-8$, 18). The small clusters with $n = 4-8$ are found to be the most stable in the nearly square-planar four-coordinate configuration, except for $[Cu(OH)_3(H_2O)]^-$, which is three-coordinate. In the presence of the two full hydration shells ($n = 18$), however, the five-coordinate square-pyramidal geometry is the most favorable for $Cu(MeNH_2)^{2+}$ (5, 6) and $Cu(OH)^+$ (5, 4, 6), and the four-coordinate geometry is the most stable for $Cu(OH)_2$ (4, 5) and $Cu(OH)_3^-$ (4). (Other possible coordination numbers for these complexes in the aqueous phase are shown in parentheses.) A small energetic difference between these structures (0.23−2.65 kcal/mol) suggests that complexes with different coordination numbers may coexist in solution. Using two full hydration shells around the Cu^{2+} ion (18 ligands) gives Gibbs free energies of aqueous reactions that are in excellent agreement with experiment. The mean unsigned error is 0.7 kcal/mol for the three consecutive hydrolysis steps of Cu^{2+} and the complexation of Cu^{2+} with methylamine. Conversely, calculations for the complexes with only one coordination shell (four equatorial ligands) lead to a mean unsigned error that is >6.0 kcal/mol. Thus, the explicit treatment of the first and the second shells is critical for the accurate prediction of structural and thermodynamic properties of Cu(II) species in aqueous solution.

1. Introduction

Copper is a key component of many metalloenzymes involved in the activation of various biochemical processes, including electron and oxygen transport, oxidative cleavage of biogenic amines, reduction of nitrogen oxides, and insertion of molecular oxygen into a substrate.[1−7] It was suggested that Cu^{2+} and several other dications could act as catalysts for the formation of peptide bonds in aqueous solution.[8,9] Cu^{2+} can readily move across cell membranes and through ion channels and become toxic at elevated cellular concentrations.[10] There is some evidence that copper may be involved in the pathogenesis of atherosclerosis, Alzheimer's diseases, and other neurodegenerative diseases of aging.[11] Similar to the classic Fenton chemistry in aqueous solution, a redox-active copper ion generates reactive oxygen species (i.e., hydroxyl radical) that can cause oxidative damage to various molecules.

Knowledge of the local coordination environment around Cu^{2+} in aqueous solutions is critical for understanding the biological functions of copper and copper-containing proteins. The electronic term of Cu^{2+} in the regular octahedral geometry is 2-fold degenerate, and according to the Jahn−Teller theorem,[12,13] it has no minimum with respect to certain nuclear displacements. Distortion of the octahedral geometry occurs along one of the three 4-fold axes. One of the important consequences of the Jahn−Teller effect is a variability of the coordination geometry of Cu^{2+} in the solid state[14−21] and the fast first-shell ligand exchange dynamics in the aqueous phase.[22,23] Surprisingly, the coordination environment even for the simplest hydrated Cu(II) ion has been the subject of extensive debate in recent years.[21,24−32] The most recent X-ray absorption studies (EXAFS and XANES) of aqueous solution of Cu(II),[26] as well as theoretical calculations performed by us[30] and others,[31,32] showed that the $[Cu(aq)]^{2+}$ ion can be represented as a five-coordinate square-pyramidal structure with one elongated axial water molecule. Despite the flexibility of the coordination geometry, Cu^{2+} is one of the most strongly coordinated divalent transition metal ions. It has the highest hydration free energy and the largest complexation free energy for aliphatic N-containing ligands among the first-row transition-metal ions with the same charge.[33] This is due to a combination of several factors, including high electron affinity, small ionic radius, and large ligand field stabilization energy.

The coordination chemistry of Cu^{2+} with ligands containing N and O donors has a significant effect on its fate, transport, and reactivity in biological and environmental systems. To date, the majority of electronic structure calculations of Cu(II) complexation in aqueous solution have only provided explicit treatment of the first coordination shell.[17,34−39] The effect of a full second hydration shell on the structure and energetics of copper(II)−ligand complexes has not been considered in much detail before.

The hydrated Cu^{2+} ion is the predominant species in aqueous solution at pH < 7, while the mono and polynuclear hydroxido complexes are formed in appreciable amounts at pH ≥ 7.[33,40] The hydrolysis reactions of Cu^{2+} ($Cu^{2+} + H_2O = CuOH^+ + H^+$; $p^*K_1 = -\log^*K_1 = 7.9$) are critical to understanding the speciation of the Cu^{2+}−hydroxide complexes in natural water systems and alkaline solutions of industrial importance. In the gas phase, $[Cu(OH)(H_2O)_n]^+$ can be produced from

* Corresponding author. Phone: 626 395 2730. Fax: 626 585 0918. E-mail: slava@wag.caltech.edu, wag@wag.caltech.edu.

10.1021/jp904816d CCC: $40.75
Published on Web 08/05/2009

$[Cu(H_2O)_{n+k}]^{2+}$ via unimolecular charge separation ($n = 2-4$) and electron capture dissociation ($n = 1-10$) reactions.[41,42]

Accurate computation of free energy changes for reactions involving transition-metal ions in the aqueous phase has proved to be particularly challenging, mainly because it requires accurate estimation of the differential effect of solvation on these reactions.[31,32,43−55] This problem can be especially severe for reactions involving a change in the charge of a metal center. Therefore, the results of calculations of reaction free energies involving transition-metal ions are highly sensitive to the choice of computational and cluster models. For example, the hydrolysis constants of $[Fe(aq)]^{3+}$ calculated from the four independent studies[43−46] differ by more than 10 p*K* units. Recent successes in predicting reaction free energies in aqueous solutions have been attributed for the most part to a compensation of errors in the applied cluster/continuum model, density functional, and the basis set.[46−48] Therefore, the development of a strategy that enables systematic improvements of the calculated reaction free energies with increasing level of theory and cluster size would be an important milestone in our search for more accurate computational methods for systems involving strongly solvated transition-metal complexes.

In this paper, we extend our previous theoretical work[30] of Cu^{2+} hydration to the complexation of Cu^{2+} with methylamine and the hydrolysis reactions of Cu^{2+}. More specifically, we focus on the structures of these Cu^{2+} complexes and the accurate evaluations of reaction free energies (equilibrium constants) in aqueous solutions. We use density functional theory (DFT) calculations with a COSMO continuum solvent model[56] to determine the geometries and relative energies of $[Cu(MeNH_2)(H_2O)_{n-1}]^{2+}$ and $[Cu(OH)_x(H_2O)_{n-x}]^{2-x}$ complexes as a function of cluster size, with $n = 4-8$, 18 and $x = 1-3$. In all cases, we evaluate the effect of a full second hydration shell on the geometries and energetics of the copper−methylamine and copper−hydroxide complexes.

2. Computational Methods

Electronic structure calculations were performed using the Turbomole 5.7 quantum chemistry software.[57] DFT calculations were carried out using Becke's[58] three-parameter functional and the correlation function of Lee, Yang, and Parr[59] (B3LYP). The application of the B3LYP to metal ion−water systems has met with reasonable success.[38,60−62] Previous calculations for Cu(II)−water complexes showed that B3LYP provides a reliable description of cluster geometries, energies, and IR spectra.[30,42] The standard 6-311++G(d,p) basis set with diffuse functions was employed for the light atoms. This combination of theory and basis set provides nearly optimal performance for predicting binding energies of large $(H_2O)_{20}$ clusters.[63] The standard Los Alamos effective core potential (ECP) LACVP[64] uncontracted to form a triple-ζ valence basis set, LACV3P,[65] and augmented by the diffuse function ($\alpha_d = 0.07$) was employed for Cu. We checked the accuracy of the pseudopotential treatment of Cu by comparing with the all-electron calculations employing the TZVP basis set and the diffuse function ($\alpha_d = 0.07$) on Cu. Test calculations for the five- and six-coordinate isomers of $[Cu(OH)(H_2O)_{17}]^+$ and four- and five-coordinate isomers of $[Cu(OH)_2(H_2O)_{16}]$ showed that the use of the ECP approximation leads to only small changes in bond lengths (root mean squared deviation of 0.004 and 0.070 Å for equatorial and axial bonds, respectively) and relative energies (0.06−0.26 kcal/mol) without affecting the metal coordination structure. The overall good agreement thus justifies the subsequent use of the LACV3P ECP for Cu. To assess the effect of basis set size, we also performed single-point energy calculations using the LACV3P+ basis set augmented by two f-polarization functions[66] ($\alpha_f = 4.97$ and 1.30) on Cu and the 6-311++G(3df,3pd) basis set on the light atoms. A number of additional calculations (single-point energy on the optimized B3LYP/LACV3P+/6-311++G(d,p) geometries) were performed within the generalized-gradient approximation using the PBE,[67] PB86,[58,68] and BLYP[58,59] functionals. Vibrational frequencies were computed analytically at the B3LYP/LACVP/6-31G(d,p) level using the Jaguar 7.5 program package.[69] The standard Gibbs free energy of each species optimized in the gas phase was calculated using the rigid rotor−harmonic oscillator approximation without scaling.

Solvation calculations were carried out using the COSMO dielectric continuum model[56] implemented in Turbomole,[57] with geometries fully optimized in the solvent reaction field at the B3LYP/LAV3P+/6-311++G(d,p) level. COSMO calculations were carried out using the recommended solvation parameters optimized for neutral solutes:[70] solvent probe radius of 1.3, solvent dielectric constant of 78.4, and atomic radii of 1.30 Å for hydrogen and 1.72 Å for oxygen. The Bondi radius,[71] scaled by 1.17 (2.223 Å), was used for copper. The results are not sensitive to the choice of this parameter if the metal ion is completely surrounded by water molecules. The surface-area-dependent nonpolar solvation contributions[72] due to a relatively small effect on the reaction and relative conformation energies were not included in the solvation calculations. For instance, the difference in the estimated cavity formation terms for the four- and six-coordinate $[Cu(OH)(H_2O)_{17}]^+$clusters is less than 0.05 kcal/mol.

3. A Mixed Cluster/Continuum Model for Transition Metal Ion Complexes in Aqueous Solutions

The solvation of aqueous Cu^{2+} complexes was modeled by explicit inclusion of water molecules in the vicinity of the metal ion and implicit treatment of the rest of the solvent with dielectric continuum models. Such mixed cluster/continuum models (supermolecular approaches)[30,73] are preferred over pure dielectric continuum models when dealing with ionic solutes that have concentrated charge densities. Mixed solvation models explicitly include chemically important solute−solvent interactions and account for charge transfer to the solvent that are particularly important for hydrated transition-metalion complexes.[73−76]

The use of mixed cluster/continuum solvation models has been the subject of some criticisms,[77] including the incorrect orientations of water molecules near the dielectric boundary and the accurate evaluation of the entropic effects for the explicit water molecules. The first problem can be alleviated by the addition of a full first or second solvation shell. This will avoid the placement of loosely bound solvent molecules with arbitrary orientations. The second problem has been insufficiently appreciated in the literature and we concur with the criticism that the inclusion of explicit water molecules in a continuum calculation could be troublesome in some cases when the model is used improperly.[73] A key assumption of continuum models is that the solute is considered as rigid species with no solvent-induced change of its internal partition function. This assumption is appropriate for small rigid molecules, but it is not valid for hydrogen-bonded complexes due to their high mobility in solution and the diffusion of water molecules inside a cluster.[78] Therefore, the use of a mixed solvation model would tend to underestimate the solvation free energy of a supermolecular species. Nevertheless, it is usually possible to alleviate this problem using hydrogen-bonded complexes of similar size on both sides of the thermodynamic cycle/reaction of interest.[73]

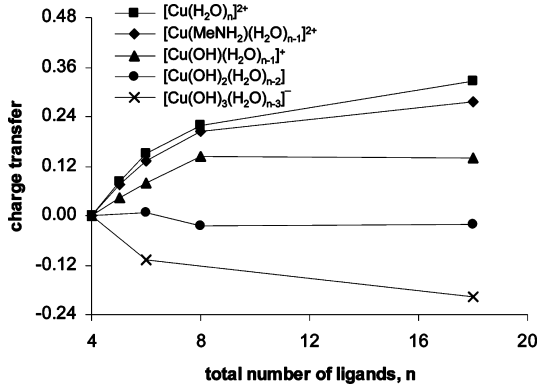

Figure 1. The dependence of the charge transfer (the natural atomic orbital charge) between the first shell equatorial ligands bonded to the Cu^{2+} ion and the outer shell water molecules on the ligand type and cluster size.

The presence of the full second shell has the effect of preventing a strong overpolarization of the first shell due to the redistribution of the total polarization energy among a much larger number of molecules. Additionally, a substantial amount of the polarization energy is included explicitly through the charge transfer effect.[73−76] Indeed, as illustrated in Figure 1 (using charges from natural atomic orbitals), there is a significant charge transfer between the first shell equatorial ligands and the second shell water molecules of various Cu^{2+}clusters with nonzero total charge. As expected, the extent of charge transfer and the rate of its convergence as a function of cluster size strongly depend on the total charge of the system. For example, the change in the extent of charge transfer for $[Cu(OH)(H_2O)_{n-1}]^+$ (0.007e) and $[Cu(OH)_2(H_2O)_{n-2}]$ (0.004e) is very small for $n = 8-18$. However, it is still significant for the $[Cu(H_2O)_n]^{2+}$ (0.107e) and $[Cu(MeNH_2)(H_2O)_{n-1}]^{2+}$ (0.073e). Continuum dielectric models and classical molecular dynamics simulations with nonpolarizable potentials do not permit a proper treatment of charge transfer effects. Thus, explicit quantum mechanical modeling of the second hydration shell around divalent transition-metal ions is critical for accurate predictions of their complexation properties in aqueous solutions. For trivalent and more highly charged metal ions, it might be necessary to use more extended hydration layers.

4. Results and Discussion

First, we carried out a search of the low-energy conformers of $[Cu(MeNH_2)(H_2O)_{n-1}]^{2+}$ and $[Cu(OH)_x(H_2O)_{n-x}]^{2-x}$ ($n = 4-8$, 18, $x = 1-3$), both in the gas phase and in the COSMO solvent reaction field. For clusters with $n \leq 8$, a thorough systematic search of the plausible low-energy structures was performed. For clusters with $n = 18$, all possible structures formed by substitution of $MeNH_2$ and OH^- for equatorial water molecules in $[Cu(H_2O)_{18}]^{2+}$ (Figure 2) were considered in order to determine the lowest energy isomer for each cluster composition and metal coordination number. Figures 2−6 show the structures and relative energies of the most stable complexes for each cluster size. The average Cu−ligand distances for the lowest energy structures of the fully hydrated Cu(II) complexes ($n = 18$) in the aqueous phase are summarized in Table 1. The calculated energies of these complexes are given in Table 1S of the Supporting Information. Table 2 lists the calculated free energies of complexation of Cu^{2+} with methylamine. Table 3 lists the calculated free energies of hydrolysis of Cu^{2+}. Finally, in Tables 4, 5, and 2S (Supporting Information) we highlight the effects of density functional, basis set, and cluster model

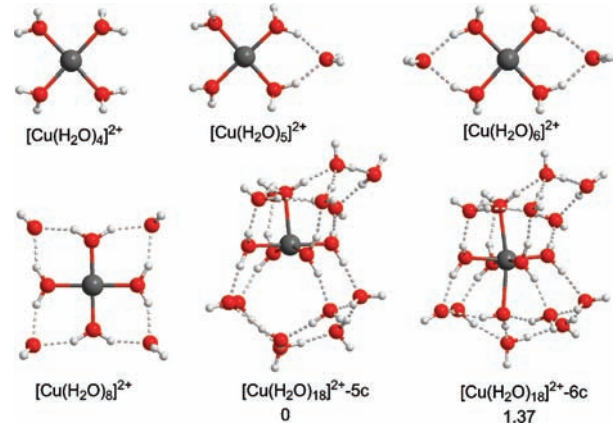

Figure 2. Structures and relative energies (kcal/mol) of $[Cu(H_2O)_n]^{2+}$ optimized in the field of the continuum solvent (COSMO model) at the B3LYP/LACV3P+/6-311G++(d,p) level of theory. $[Cu(H_2O)_{18}]^{2+}$-5c is only stable in solution and converts to $[Cu(H_2O)_{18}]^{2+}$-6c in the gas phase.

TABLE 1: Average Cu−Ligand Distances (Å) for the Lowest Energy Cu(II) Complexes in the Aqueous Phase[a]

complex	cn[b]	$r_{Cu-N(amine)/OH^-}$	r_{Cu-Oeq}	r_{Cu-Oax}
$[Cu(H_2O)_{18}]^{2+}$-5c	5		2.001 (0.008)	2.272
$[Cu(MeNH_2)(H_2O)_{18}]^{2+}$-5c	5	2.017	2.029 (0.015)	2.272
$[Cu(OH)(H_2O)_{17}]^{+}$-5c	5	1.918	2.033 (0.005)	2.361
$[Cu(OH)_2(H_2O)_{16}]$-*cis*-4c	4	1.930(0.006)	2.026 (0.006)	
$[Cu(OH)_3(H_2O)_{15}]^{-}$-4c	4	1.951(0.008)	2.062	

[a] The structures of the complexes are shown in Figures 2−6. The root mean squared deviations from the mean bond length are given in parentheses. [b] Coordination number.

TABLE 2: Complexation Free Energies of Cu^{2+} with Methylamine in the Aqueous Phase Calculated Using the Thermodynamic Cycle Shown in Scheme *1* (kcal/mol)

			$\Delta G^*_{compl,aq}$[a]	
n	$\Delta G^\circ_{compl,g}$	$\Delta\Delta G^*_{solv}$	calc	expt[b]
4	−24.08	7.19	−14.51	
5	−21.23	5.57	−13.28	
6	−20.41	5.89	−12.15	
8	−13.97	2.18	−9.41	
18	−7.06	−0.90	−5.58	
bulk limit				−5.61 ± 1.00

[a] $\Delta G^*_{compl,aq}$ is determined by eq 1a. [b] Reference 81.

on the calculated free energies of Cu^{2+} complexation and hydrolysis in aqueous solutions.

4.1. Geometries. ***4.1.1. $[Cu(H_2O)_n]^{2+}$.*** We have previously investigated the structure and energetics of various hydrated Cu^{2+} complexes.[30] The lowest-energy structures of $[Cu(H_2O)_n]^{2+}$ in the aqueous phase for $n = 4-8$ and 18 are depicted in Figure 2. Consistent with recent EXAFS and NEXAFS studies of Cu^{2+}−water complexes,[26] our calculations predict the five-coordinate $[Cu(H_2O)_{18}]^{2+}$-5c cluster to be slightly more stable than the six-coordinate $[Cu(H_2O)_{18}]^{2+}$-6c form in solution. However, in the gas phase, $[Cu(H_2O)_{18}]^{2+}$-5c is not stable and reverts to $[Cu(H_2O)_{18}]^{2+}$-6c. Note that a metal ion−water cluster with 18 water molecules and S_6 symmetry ($[M(H_2O)_{18}]^{2+/3+}$-S_6) has been recently reported as the lowest-energy minimum for Mg^{2+}, Al^{3+}, and a series of transition-metal ions.[51,54,79] For Cu^{2+} we found that a cluster of this type is only marginally more stable (by 1.4 kcal/mol) than the $[Cu(H_2O)_{18}]^{2+}$-6c isomer shown in Figure 2 Furthermore, the inclusion of zero-point energy, solvation, and thermal corrections at 298 K makes these two types of stable clusters essentially isoenergetic, with the

TABLE 3: Gibbs Free Energies of the Hydrolysis Reactions of Cu^{2+} Calculated Using the Thermodynamic Cycle Shown in Scheme *2* (kcal/mol)

			$\Delta G^*_{x,\mathrm{hydr,aq}}$[a]	
n	$\Delta G^\circ_{x,\mathrm{hydr,g}}$	$\Delta\Delta G^*_{\mathrm{solv}}$	calc	expt[b]
	$[Cu(H_2O)_n]^{2+} = [Cu(OH)(H_2O)_{n-1}]^+ + H^+$			
4	119.51	−126.52	−5.12	
5	130.45	−136.30	−3.96	
6	139.26	−144.13	−2.98	
8	158.64	−160.53	0.00	
18	188.12	−186.01	3.99	
bulk limit				10.85 ± 0.28
	$[Cu(OH)(H_2O)_{n-1}]^+ = [Cu(OH)_2(H_2O)_{n-2}] + H^+$			
4	221.01	−217.28	5.61	
6	224.13	−221.51	4.51	
8	230.90	−225.00	7.79	
18	248.06	−243.03	6.93	
bulk limit				11.25 ± 0.28
	$[Cu(OH)_2(H_2O)_{n-2}] = [Cu(OH)_3(H_2O)_{n-3}]^- + H^+$			
4	319.78	−309.97	11.70	
6	326.32	−313.56	14.65	
18	302.19	−295.72	8.36	
bulk limit				14.19 ± 0.28

[a] $\Delta G^*_{x,\mathrm{hydr,\ aq}}$ is determined by eq 2a. [b] Reference 40.

TABLE 4: Relative Energies of $[Cu(OH)(H_2O)_{17}]^+$ and $[Cu(OH)_2(H_2O)_{16}]$ Complexes in Aqueous Solution Obtained with Various DFT Methods (kcal/mol)[a]

	$[Cu(OH)(H_2O)_{17}]^+$		$[Cu(OH)_2(H_2O)_{16}]$	
DFT	5-coord	6-coord	4-coord	5-coord
B3LYP	0	2.23	0	0.98
BPE	0	2.58	0	1.68
BP86	0	2.94	0	1.98
BLYP	0	3.32	0	2.82

[a] LACV3P+/6-311G++(d,p) single point energies on B3LYP/LACV3P+/6-311G++(d,p) optimized geometries. Solvation effects are included at the COSMO-B3LYP/LACV3P+/6-311G++(d,p) level.

$[Cu(H_2O)_n]^{2+}$-5c isomer being now slightly more stable by 0.2 kcal/mol. We subsequently used the $[Cu(H_2O)_{18}]^{2+}$-5c cluster as a model cluster for water replacement by $MeNH_2$ and OH^-, because it can accommodate a broad range of coordination numbers (4, 5, and 6). Note that due to the specific arrangement of hydrogen bonds, the family of $[M(H_2O)_{18}]^{2+}$-S_6 clusters is only suitable to study systems with the six-coordinate geometry. Indeed, as reported in ref 81, substitution of Mg^{2+} by Li^+ and Be^{2+} in $[Mg(H_2O)_{18}]^{2+}$-S_6 and reoptimization of the geometry did not alter the coordination number, even though these metal ions are more stable in a tetrahedral environment.

4.1.2. $[Cu(MeNH_2)(H_2O)_{n-1}]^{2+}$. We examined all possible structures generated by replacement of nonequivalent equatorial water molecules in $[Cu(H_2O)_n]^{2+}$ by methylamine. The structures of the lowest-energy conformers in the aqueous phase for n = 4−8 and 18 are shown in Figure 3. Water is a stronger hydrogen-bond donor than methylamine. Therefore, the fifth and the sixth water ligands prefer to form two hydrogen bonds with the first-shell water molecules. The two subsequent water molecules are bonded to the equatorial water and amine in a similar arrangement, while the axial copper(II) sites are energetically less favorable for clusters of this size. Similar to the hydrated Cu(II) species, the $[Cu(MeNH_2)(H_2O)_{17}]^{2+}$-5c is only stable in the aqueous phase. The conformer with the two axial waters ($[Cu(MeNH_2)(H_2O)_{17}]^{2+}$-6c) is 2.65 kcal/mol higher in energy in aqueous solution. Comparing this value to that of $[Cu(H_2O)_{18}]^{2+}$ (1.37 kcal/mol), we note that the presence of a stronger σ-donor ligand causes a greater stabilization of the five-coordinate cluster geometry.

4.1.3. $[Cu(OH)(H_2O)_{n-1}]^+$. The structures and relative energies of the most stable $[Cu(OH)(H_2O)_{n-1}]^+$ complexes in the aqueous phase for different coordination numbers are depicted in Figure 4. The strongly coordinated OH^- ligand acts as a hydrogen-bond acceptor, forming one or two hydrogen bonds with water molecules in the second shell. On the basis of the relative energies of the $[Cu(OH)(H_2O)_4]^+$-4c-A and $[Cu(OH)(H_2O)_4]^+$-4c-B isomers, we find that the strength of this interaction is comparable or slightly less than that of a hydrogen bond in systems with equatorial water molecules. In contrast, the hydrogen-bond-donor ability of the OH^- group is relatively weak, as it forms no hydrogen bonds with water molecules in the most stable water clusters with n = 4−18. For smaller clusters (n = 4−8), we find a strong preference for a four-coordinate arrangement. For example, the quasiplanar geometry of $[Cu(OH)(H_2O)_7]^+$ is energetically preferred by 2.47 and 7.44 kcal/mol compared to the corresponding structures with one and two axial waters. When a full second hydration shell is included, the five-coordinate cluster becomes the most stable both in the gas and solution phases. However, the differences in the solution-phase energies of the stable four-, five-, and six-coordinate $[Cu(OH)(H_2O)_{17}]^+$ cluster geometries are quite small (within 2.2 kcal/mol), thereby suggesting that they may dynamically coexist in solution.

4.1.4. $[Cu(OH)_2(H_2O)_{n-2}]$. Figure 5 shows the lowest-energy cis and trans isomers of the four-coordinate $[Cu(OH)_2(H_2O)_{n-2}]$ complexes with n = 4, 6, and 8. The trans form is more stable in the gas phase, while the cis form is more stable in the aqueous phase. The exception is for the $[Cu(OH)_2(H_2O)_6]$-*cis* conformer, which has a much higher energy in the gas phase than the trans conformer. We ascribe this difference to weak hydrogen bonding between the oxygen atoms of the water molecules and the

TABLE 5: Comparison of the Gibbs Free Energies of Aqueous Reactions Obtained with Various DFT Methods and Basis Sets (kcal/mol) Using Two Full Hydration Shells around the Cu^{2+} Ion (18 Ligands)[a]

	BLYP		BP86		PBE		B3LYP			
	BS1	BS2	BS1	BS2	BS1	BS2	BS1	BS2	BS1(corr)[b]	expt
$\Delta G^*_{\mathrm{compl,aq}}$	−7.04	−7.53	−6.68	−7.16	−7.82	−8.19	−5.58	−5.93	−5.58	−5.61
$\Delta G^*_{1,\mathrm{hydr,aq}}$	−2.65	−3.34	−1.43	−2.20	−1.34	−2.21	4.00	3.25	9.66	10.85
$\Delta G^*_{2,\mathrm{hydr,aq}}$	0.87	−0.33	1.39	0.12	1.53	0.15	6.93	5.66	12.60	11.25
$\Delta G^*_{3,\mathrm{hydr,aq}}$	4.71	4.53	4.95	4.80	4.87	4.65	8.36	8.20	14.02	14.19
MUE[c]	8.70	9.34	8.12	8.77	8.36	9.07	4.26	4.88	0.68	

[a] BS1 is the LACV3P+/6-311G++(d,p) basis set. BS2 is the LACV3P+(2f)/6-311G++(3df,3pd) basis set. Single point energies on B3LYP/LACV3P+/6-311G++(d,p) optimized geometries. Solvation effects are included at the COSMO-B3LYP/LACV3P+/6-311G++(d,p) level. [b] Using a constant empirical correction term to minimize the systematic errors in the calculated hydrolysis constants. [c] MUE denotes mean unsigned error (also called mean absolute error) for the complexation and three hydrolysis reactions.

SCHEME 1: Thermodynamic Cycle for the Calculation of the Complexation Free Energies (Stability Constants) of Cu(II) with $MeNH_2$ in Water

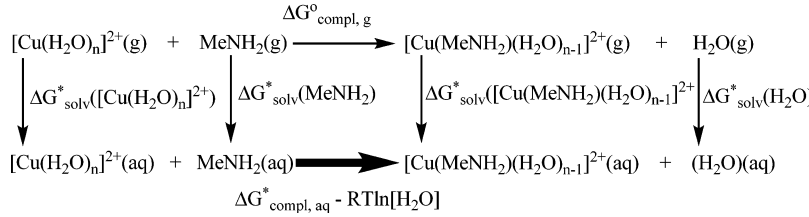

SCHEME 2: Thermodynamic Cycle for the Calculation of the Deprotonation Free Energies (Hydrolysis Constants) of Cu(II) Hydrate

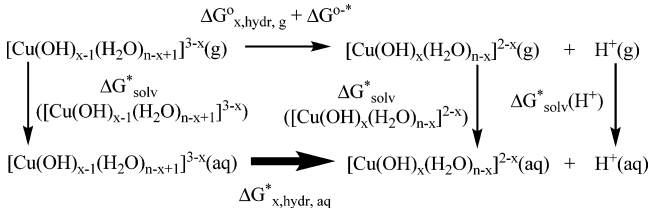

hydrogen atoms of the hydroxide ions. Poorer solvation of the trans form could be attributed to its negligible or small dipole moment (0−0.8 D) compared to that of the corresponding cis isomers (1.9−6.2 D). In the presence of two full hydration shells, the square-planar complex remains the most stable in the aqueous phase, whereas the square pyramidal complex is marginally more stable in the gas phase. We did not find a stable dihydroxide copper(II) cluster coordinated to six ligands.

4.1.5. $[Cu(OH)_3(H_2O)_{n-3}]^-$. We also investigated the structure and energetics of $[Cu(OH)_3(H_2O)_{n-3}]^-$ complexes with $n = 4$, 6, and 18. The lowest-energy structures are shown in Figure 6. The $[Cu(OH)_3(H_2O)]^-$ species with an equatorial water is not a minimum on the potential energy surface. Geometry optimization yields a three-coordinate Cu^{2+} complex, with the water molecule migrated to the second shell. Conversely, a square-planar geometry is the only stable arrangement for the larger $[Cu(OH)_3(H_2O)_3]^-$ and $[Cu(OH)_3(H_2O)_{15}]^-$ clusters. The data in Table 1 confirm the monotonic increase of the average Cu(II)−OH distance with the number of OH^- ligands as typically observed in metal ion coordination complexes.

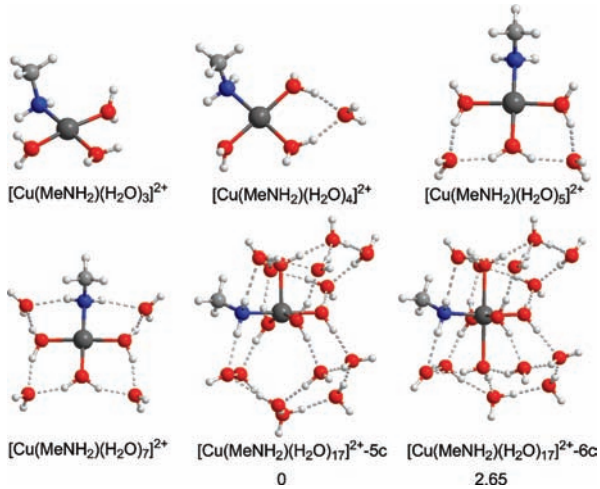

Figure 3. Structures and relative energies (kcal/mol) of $[Cu(MeNH_2)H_2O)_{n-1}]^{2+}$ optimized in the field of the continuum solvent (COSMO model) at the B3LYP/LACV3P+/6-311G++(d,p) level of theory. $[Cu(MeNH_2)(H_2O)_{17}]^{2+}$-5c is only stable in solution and converts to $[Cu(MeNH_2)(H_2O)_{17}]^{2+}$-6c in the gas phase.

4.2. Free Energies of Cu^{2+} Complexation and Hydrolysis in Aqueous Solutions. ***4.2.1. Methylamine Complexation.*** Complexation free energies are calculated using the thermodynamic cycle shown in Scheme 1. From Scheme 1, $\Delta G^*_{compl,aq}$ can be expressed as a sum of the gas-phase free energy of complexation ($\Delta G^\circ_{compl,g}$), the differential solvation free energy for a given reaction ($\Delta\Delta G^*_{solv}$), and the concentration correction term

$$\Delta G^*_{compl,\,aq} = \Delta G^\circ_{compl,g} + \Delta\Delta G^*_{solv} + RT\ln([H_2O]) \quad (1a)$$

$$\Delta\Delta G^*_{solv} = \Delta G^*_{solv}([Cu(MeNH_2)(H_2O)_{n-1}]^{2+}) + \Delta G^*_{solv}(H_2O) - \Delta G^*_{solv}([Cu(H_2O)_n]^{2+}) - \Delta G^*_{solv}(MeNH_2) \quad (1b)$$

Here, $RT\ln([H_2O]) = 2.38$ kcal/mol is a free energy change of 1 mol of H_2O gas from 55.34 M liquid state to 1 M standard state in solution. This conversion factor needs to be included when water is one of the reacting species in the aqueous phase.[73,78,81]

Table 2 summarizes the calculated free energies of complexation of methylamine with Cu(II) in the aqueous phase as a function of n. The gas phase and solvation contributions are also given for comparison. The calculated complexation free energies monotonically decrease in absolute value and start to level off as n increases. The change in $\Delta G^*_{compl,aq}$ is moderately large from $n = 4$ to 8 (∼1.3 kcal/mol per water molecule) and relatively small from $n = 8$ to 18 (∼0.4 kcal/mol per water molecule). The results are expected to be reasonably converged at $n = 18$. In this case, the contribution from $\Delta\Delta G^*_{solv}$ is smaller than 1 kcal/mol. For $n = 18$, the calculated free energy of complexation of Cu^{2+} with methylamine (−5.58 kcal/mol) is in excellent agreement with the experimental value (−5.61 ± 1.00 kcal/mol).[80] Conversely, the use of a cluster model with only four equatorial ligands leads to an overestimation of the complex stability by almost 9 kcal/mol. These results strongly support the need to include full second hydration shells when using cluster/continuum models to calculate the complexation free energies of transition-metal ions such Cu(II) in aqueous solutions.

4.2.2. Hydrolysis Reactions. The Gibbs free energies of the three hydrolysis reaction steps of Cu^{2+} are calculated using the thermodynamic cycle shown in Scheme 2. In this case, $\Delta G^*_{x,hydr,aq}$ for the xth hydrolysis reaction step can be written as a sum of the gas-phase deprotonation energy ($\Delta G^\circ_{x,hydr,g}$), the differential solvation free energy ($\Delta\Delta G^*_{solv}$), and the standard state correction term ($\Delta G^{\circ\rightarrow *}$)

$$\Delta G^*_{x,\mathrm{hydr,aq}} = \Delta G^\circ_{x,\mathrm{hydr,g}} + \Delta\Delta G^*_{\mathrm{solv}} + \Delta G^{\circ\rightarrow *} \quad (2a)$$

$$\Delta\Delta G^*_{\mathrm{solv}} = \Delta G^*_{\mathrm{solv}}([\mathrm{Cu(OH)}_x(\mathrm{H_2O})_{n-x}]^{2-x}) + \Delta G^*_{\mathrm{solv}}(\mathrm{H^+}) - \Delta G^*_{\mathrm{solv}}([\mathrm{Cu(OH)}_{x-1}(\mathrm{H_2O})_{n-x+1}]^{3-x}) \quad (2b)$$

Here, $\Delta G^{\circ\rightarrow *} = RT \ln(24.46) = 1.89$ kcal/mol ($T = 298.15$ K) is a standard state correction factor.[73,82] For the solvation free energy of the proton, $\Delta G^*_{\mathrm{solv}}(\mathrm{H^+})$, we used the recommended value[83] of -265.9 ± 3.0 kcal/mol derived by Tissandier et al.[84] and recently reproduced by Kelly et al.[82] using the cluster-pair approximation. Note that we have recently calculated the solvation free energy of the proton using the mixed cluster/continuum model and obtained a value of -266.7 kcal/mol.[73] The computed value is very close to the recommended one and will not significantly alter the calculated hydrolysis free energies.

The calculated free energies for the three hydrolysis reaction steps of Cu^{2+} are listed in Table 3. Note that calculated gas-phase deprotonation free energies and the differences in solvation free energy involving hydrolysis reactions are often very large numbers ($\sim$120$-$320 kcal/mol) that enter eq 2a with opposite signs. Therefore, the accurate prediction of $\Delta G^*_{\mathrm{hydr,aq}}$ is a difficult task and will depend to some extent on compensation of errors.[46−48] Note that the calculated $\Delta G^*_{1,\mathrm{hydr,aq}}$ values exhibit a systematic dependence on cluster size, increasing by 9.1 kcal/mol from $n = 4$ to 18. In contrast, a smaller variation is observed for $\Delta G^*_{2,\mathrm{hydr,aq}}$ which increases by only 1.3 kcal/mol from $n = 4$ to 18. However, $\Delta G^*_{3,\mathrm{hydr,aq}}$ again shows a large variation with n, thereby requiring a quantum mechanical treatment of the full second hydration shell to achieve reasonably converged results in solutions. Such variability in $\Delta G^*_{x,\mathrm{hydr,aq}}$ may not be surprising, because the convergence of the hydration free energies of $CuOH^+$ and $Cu(OH)_2$ species with cluster size occurs at a faster rate compared to that of the doubly charged Cu^{2+} and negatively charged (and more polarizable) $Cu(OH)_3^-$ ions. This is further illustrated in Figure 1 by the variation of charge transfer in $[\mathrm{Cu(OH)}_x(\mathrm{H_2O})_{n-x}]^{2-x}$ as a function of cluster size. Table 3 indicates that the calculated $\Delta G^*_{\mathrm{hydr,aq}}$ are systematically underestimated compared to experimental values by 5$-$7 kcal/mol, even with the inclusion of a full second hydrations shell. We discuss this discrepancy in the next section.

4.2.3. Effects of DFT Functional, Basis Set, and Solvent Model on the Calculated Free Energy Changes in Aqueous Reactions. First, we examined the effect of DFT exchange-correlation functional on the relative stability of conformational isomers. Table 4 compares relative total energies in aqueous solution for the two conformers of $[\mathrm{Cu(OH)(H_2O)_{17}}]^+$ and $[\mathrm{Cu(OH)_2(H_2O)_{16}}]$ using the PBE, BP86, BLYP, and B3LYP functionals. These DFT methods were selected given their widespread use and reasonable performance for transition-metal ion$-$water systems.[31,32,46−48,51,52] The results indicate that variation of the DFT functional used does not lead to qualitative changes in the stability of clusters in the aqueous phase, with the square-pyramidal and square-planar geometry being favored for $Cu(OH)^+$ and $Cu(OH)_2$, respectively. Within this series, BLYP shows the strongest tendency to stabilize the species with lower coordination numbers, while B3LYP exhibits a greater tendency to stabilize the complexes with higher coordination numbers.

Table 5 compares the performance of the four density functionals using two different basis sets. The Gibbs free energies of Cu^{2+} complexation and hydrolysis reactions were computed using the lowest-energy clusters with full second hydration shells (18 ligands). The accuracy of each method is characterized by the mean unsigned error (MUE) listed in the last row of Table 5. Overall, we find that the use of a gradient-corrected functional and a more extended basis set increases the MUE. Several factors may contribute to the systematic discrepancy between the calculated and experimental hydrolysis free energies. One source of error is the uncertainty of $\Delta G^*_{\mathrm{solv}}(\mathrm{H^+})$, which is $\geq$2 kcal/mol.[82] Another source of error could be the inaccuracy of the calculated solvation free energy contributions, which we tried to minimize by including two solvation layers. In any case, the error resulting from solvation calculations is not expected to be approximately constant for each of the three hydrolysis reaction steps.

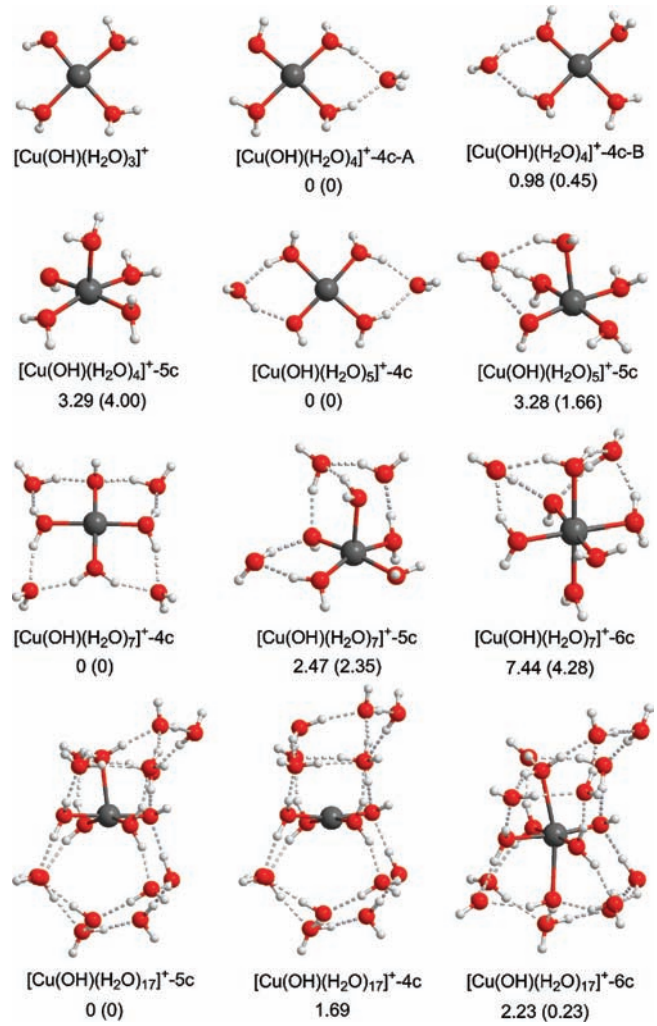

Figure 4. Structures and relative energies (kcal/mol) of $[\mathrm{Cu(OH)(H_2O)}_{n-1}]^+$ optimized in the field of the continuum solvent (COSMO model) at the B3LYP/LACV3P+/6-311G++(d,p) level of theory. Relative energies for the gas-phase optimized structures are shown in parentheses. $[\mathrm{Cu(OH)(H_2O)_{17}}]^+$-4c is only stable in solution and converts to $[\mathrm{Cu(OH)(H_2O)_{17}}]^+$-5c in the gas phase.

Static quantum chemical calculations are often performed under the assumption that the chemical potential of a solute in the gas phase and in solution is dominated by a single conformation, thus neglecting conformational entropy associated with other low-energy conformers.[44] We have not attempted to estimate the conformation entropy contribution in this study because the conformational sampling in free energy calculations can only be carried out rigorously using more computational expensive methods such as QM/MM MD[85] and CPMD.[86] However, we sought to minimize this effect by considering compact complexes with a complete (not partial) second

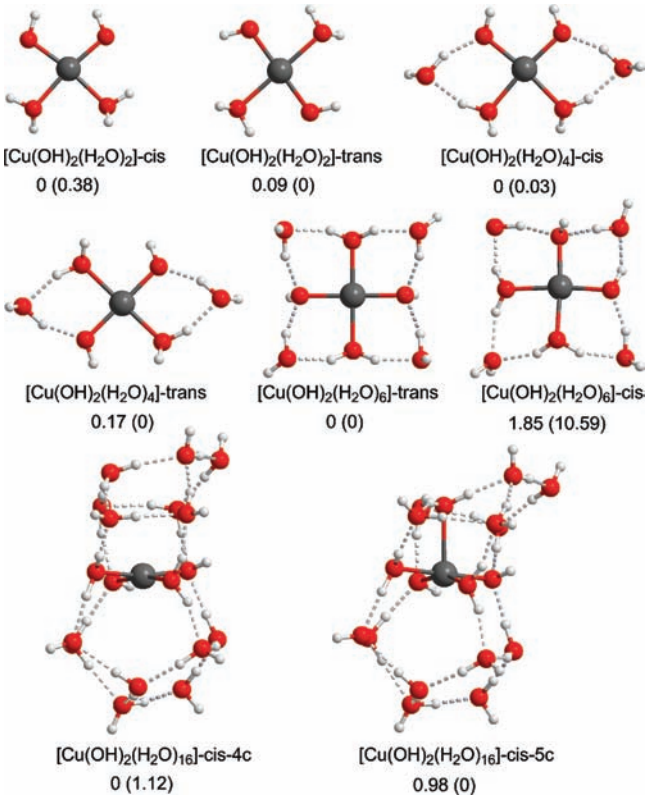

Figure 5. Structures and relative energies (kcal/mol) of $[Cu(OH)_2H_2O)_{n-2}]$ optimized in the field of the continuum solvent (COSMO model) at the B3LYP/LACV3P+/6-311G++(d,p) level of theory. Relative energies for the gas-phase optimized structures are shown in parentheses.

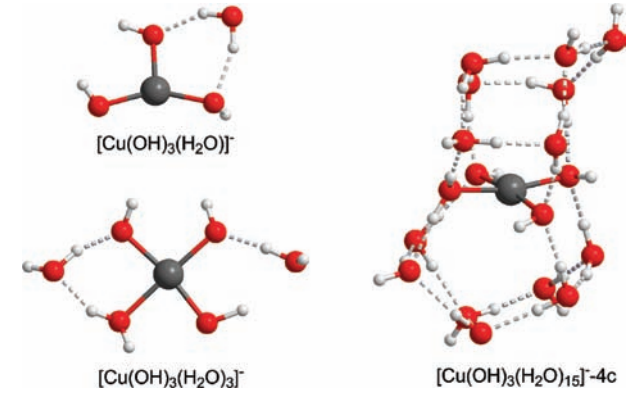

Figure 6. Structures of $[Cu(OH)_3H_2O)_{n-3}]^-$ optimized in the field of the continuum solvent (COSMO model) at the B3LYP/LACV3P+/6-311G++(d,p) level of theory.

hydration shell, which restricts the number of possible low-energy conformations. It has been suggested[44] that the conformational entropy is likely to increase progressively with decrease in the total charge of a complex, because the complexes tend to be more loosely bound and hence "less ordered". However, this would lead to free energies of the first two hydrolysis reaction steps of Cu^{2+} that are less positive than those in Table 5, thus worsening the agreement with the experimental data.

Note that our results are highly sensitive to the choice of the DFT methods, thereby suggesting that the deficiencies of the applied density functionals may be the most likely source for the systematic errors in our calculated reaction free energies. The inability of the selected density functionals to correctly predict the ionic product of water has been recently reported by Svozil et al.[87] Using the CCSD(T)/CBS energies as reliable benchmarks, they found that all tested functionals significantly overestimate the stability of the zwitterionic structure of a water octamer cluster relative to the undissociated conformer. Similarly to the results reported herein, the hybrid B3LYP functional gave more accurate energies (an error of 2.7−5.5 kcal/mol) than the gradient-corrected PBE, BP86, and BLYP functionals (an error of 6.3−11.1 kcal/mol). Svozil et al.[87] also reported that all the tested DFT functionals performed better using smaller basis sets. The fact that the smaller basis set gives better result must be related to error compensation, while the true performance of the DFT functionals is revealed using larger basis sets.

The discrepancies between calculated hydrolysis reaction free energies and experimental values with each DFT method can be reduced considerably by using a constant empirical correction term. For example, shifting the $\Delta G^*_{hydr,aq}$ values up by 5.67 kcal/mol decreases the total mean unsigned error of B3LYP from 4.26 to 0.68 kcal/mol (Table 5). Clearly, such excellent agreement with experiment is achieved through the accurate treatment of solvation effects via modeling of the second hydration shell.

An alternative way of including solvation effects for ionic solutes is to tune the default radii of atoms that define the dielectric continuum boundary so as to mimic the stabilizing effect of the second and outer hydration shells when solvent molecules are not included explicitly. This strategy is employed, for example, in the Poisson−Boltzmann (PB) continuum solvent module of the Jaguar quantum chemistry software,[65,69] which can assign atomic radii according to the chemical environment of each atom. Using Jaguar (with its PB continuum solvent model) for complexes with one coordination shell (four equatorial ligands) along with a empirically adjusted parameter for the hydrolysis constants gives a mean unsigned error of 3.5 kcal/mol (Table 2S of the Supporting Information). Although this error is 1.8 times smaller than that of the COSMO method for the Cu(II) clusters with four ligands (6.2 kcal/mol), it is 5 times larger than the error of COSMO calculations for the Cu(II) clusters with 18 ligands (0.7 kcal/mol). Furthermore, with the Jaguar solvation model, hydrolysis free energies are not predicted in the correct order. Thus, the overall results of our calculations strongly suggest that using mixed cluster/continuum models with at least two full solvation shells is critical for accurate prediction of thermodynamic properties of Cu^{2+} species in aqueous solution.

5. Conclusions

Mixed cluster/continuum models are emerging as the methods of choice for modeling the solvation and reactions of transition metal ions in aqueous solutions. We coupled density functional theory (B3LYP) with a COSMO continuum solvation model to study the geometric structure, relative energies, and thermodynamic stability of various hydrated Cu^{2+} complexes, $[Cu(MeNH_2)(H_2O)_{n-1}]^{2+}$ and $[Cu(OH)_x(H_2O)_{n-x}]^{2-x}$ ($x = 1-3$), as a function of metal−ligand coordination number (4−6) and cluster size ($n = 4-8$, 18). An extensive search of conformational space was carried out for all the complexes with $n = 4-8$. We also used a previously reported[30] structure of $[Cu(H_2O)_{18}]^{2+}$ and replaced its water molecules by methylamine and hydroxide. On the basis of the lowest-energy conformers in the aqueous phase, we estimated free energy changes for aqueous reactions involving the Cu(II) center.

The most stable complexes with $n \leq 8$ in the aqueous phase have nearly square-planar four-coordinate geometry. The exception is $[Cu(OH)_3(H_2O)]^-$, which is stable only in a three-

coordinate arrangement. In the presence of the two hydration shells around Cu^{2+}, however, we find the five-coordinate square-pyramidal geometry to be the most favorable for $Cu(MeNH_2)^{2+}$ (5, 6) and $Cu(OH)^{+}$(5, 4, 6), and the four-coordinate geometry to be the most stable for $Cu(OH)_2$ (4, 5) and $Cu(OH)_3^-$ (4). (Other possible coordination numbers for these complexes in the aqueous phase sorted in decreasing order of cluster stability are shown in parentheses.) Since the differences between the energies of the various structures are relatively small (between 0.23 and 2.65 kcal/mol), we conclude that Cu^{2+}−water/ligand clusters with different coordination numbers may coexist in solution. However, we find a general trend of decreasing coordination number with the number of OH^- ligands in the clusters. Note that the tendency to underestimate the coordination number of relatively small clusters compared to condensed-phase structures is consistent with several other studies of hydrated ions, including K^+, Ca^{2+}, and OH^-.[88−91]

We found that the explicit solvation of the first and the second shells around Cu^{2+} ($n = 18$) is needed for an accurate estimation of reaction free energies. When we use a constant empirical correction term, the mean unsigned error for three hydrolysis reaction steps of Cu^{2+} and the complexation reaction of Cu^{2+} with methylamine is small and equal to 0.7 kcal/mol. Very accurate reaction free energies are obtained due to adequate accounting for charge transfer from ligands and water to Cu^{2+} and hydrogen bonding between the equatorial ligands and surrounding water molecules. Conversely, for complexes with one coordination shell (four equatorial ligands), the mean unsigned error obtained with the Jaguar and COSMO solvation models is 3.45 and 6.14 kcal/mol, respectively. This is 5−9 times larger than the error obtained with the best model utilizing two hydration shells (18 ligands).

Acknowledgment. We are grateful to Dr. Jenny P. Glusker for providing us with the Cartesian coordinates of the $[Mg(H_2O)_{18}]^{2+}$-S_6 cluster. Funding for this work was provided by the National Science Foundation (NIRT CTS Award # 0506951) and by the US Environmental Protection Agency (STAR Grant RD-83252501). The computational facilities used in these studies were funded by grants from ARO-DURIP, ONR-DURIP, and NSF-MRI.

Supporting Information Available: Cartesian coordinates and total energies for all Cu(II) complexes optimized in the field of the continuum solvent (COSMO solvation model for water) at the B3LYP/6-311++G(d,p) level of theory, Table 1S summarizing gas-phase binding free energies and solvation free energies of Cu(II) complexes, and Table 2S showing aqueous reaction free energies calculated using complexes with one coordination shell (four equatorial ligands). This material is available free of charge via the Internet at http://pubs.acs.org.

References and Notes

(1) Adman, E. T. *Adv. Protein Chem.* **1991**, *42*, 145.
(2) Hazes, B.; Magbus, K. A.; Bonaventura, C.; Bonaventura, J.; Dauter, Z.; Kalk, K. H.; Hol, W. G. *Protein Sci.* **1993**, *2*, 597.
(3) Pufahl, R. A.; Singer, C. P.; Peariso, K. L.; Lin, S.-J.; Schmidt, P. J.; Fahrni, C. J.; Culotta, V. C.; Penner-Hahn, J. E.; O'Halloran, T. V. *Science* **1997**, *278*, 853.
(4) Culotta, V. C.; Klomp, L. W.; Strain, J.; Casareno, R. L.; Krems, B.; Giltin, J. D. *J. Biol. Chem.* **1997**, *272*, 23469.
(5) Solomon, E. I.; Szilagyi, R. K.; George, S. B.; Basumallick, L. *Chem. Rev.* **2004**, *104*, 419.
(6) MacPherson, I. S.; Murphy, M. E. P. *Cell. Mol. Life Sci.* **2007**, *64*, 2887.
(7) Brazeau, B. J.; Johnson, B. J.; Wilmot, C. M. *Arch. Biochem. Biophys.* **2004**, *428*, 22.
(8) Rode, B. M.; Suwannachot, Y. *Coord. Chem. Rev.* **1999**, *190−192*, 1085.
(9) Remko, M.; Rode, B. M. *Phys. Chem. Chem. Phys.* **2001**, *3*, 4667.
(10) Handy, R. D.; Eddy, F. B.; Baines, H. *Biochim. Biophys. Acta* **2002**, *1566*, 104.
(11) Brewer, G. I. *Exp. Biol. Med.* **2007**, *232*, 323.
(12) Jahn, H. A.; Teller, E. *Proc. R. Soc. London, Ser. A* **1937**, *161*, 220.
(13) Bersuker, I. B. *The Jahn-Teller Effect*; Cambridge University Press: Cambridge, 2006.
(14) Katz, A. K.; Shimoni-Livny, L.; Navon, O.; Bock, C. W.; Glusker, J. P. *Helv. Chim. Acta* **2003**, *86*, 1320.
(15) Halcrow, M. A. *Dalton Trans.* **2003**, 4375.
(16) Sabolovic, J.; Liedl, K. R. *Inorg. Chem.* **1999**, *38*, 2764.
(17) Sabolovic, J.; Tautermann, C. S.; Loerting, T.; Liedl, K. R. *Inorg. Chem.* **2003**, *42*, 2268.
(18) Deeth, R. J.; Hearnshaw, L. J. A. *Dalton Trans.* **2006**, 1092.
(19) Chaurin, V. C.; Constable, E. C.; Housecroft, C. E. *New J. Chem.* **2006**, *30*, 1740.
(20) Weiss, R.; Jansen, G.; Boese, R.; Epple, M. *Dalton Trans.* **2006**, 1831.
(21) Persson, I.; Persson, P.; Sandström, M.; Ullström, A.-S. *J. Chem. Soc., Dalton, Trans.* **2002**, 1256.
(22) Powell, D. H.; Helm, L.; Merbach, A. E. *J. Chem. Phys.* **1991**, *95*, 9258.
(23) Powell, D. H.; Furrer, P.; Pittet, P.-A.; Merbach, A. E. *J. Phys. Chem.* **1995**, *99*, 16622.
(24) Benfatto, M.; D'Angelo, P.; Longa, S. D.; Pavel, N. V. *Phys. Rev. B* **2002**, *65*, 174205.
(25) Chaboy, J.; Muñoz-Páez, A.; Merkling, P. J.; Marcos, E. S. *J. Chem. Phys.* **2006**, *124*, 064509.
(26) Frank, P.; Benfatto, M.; Szilagyi, R. K.; D'Angelo, P.; Longa, S. D.; Hodgson, K. O. *Inorg. Chem.* **2005**, *44*, 1922.
(27) Pasquarello, A.; Petri, I.; Salmon, P. S.; Parisel, O.; Car, R.; Tóth, É.; Powell, D. H.; Fisher, H. E.; Helm, L.; Merbach, A. E. *Science* **2001**, *291*, 856.
(28) Amira, S.; Spangberg, D.; Hermasson, K. *Phys. Chem. Chem. Phys.* **2005**, *7*, 2874.
(29) Schwenk, C. F.; Rode, B. M. *J. Am. Chem. Soc.* **2004**, *126*, 12786.
(30) Bryantsev, V. S.; Diallo, M. S.; van Duin, A. C. T.; Goddard, W. A., III. *J. Phys. Chem. A* **2008**, *112*, 9104.
(31) Blumberger, J. *J. Am. Chem. Soc.* **2008**, *130*, 16065.
(32) Blumberger, J.; Tavernelli, I.; Klein, M. L. *J. Chem. Phys.* **2006**, *124*, 64507.
(33) NIST Standard Reference Database 46. NIST Critically Selected Stability Constants of Metal Complexes: Version 8.0, May 2004, http://www.nist.gov/srd/nist46.htm.
(34) Pushie, M. J.; Rauk, A. *J. Biol. Inorg. Chem.* **2003**, *8*, 53.
(35) Prabhakar, R.; Siegbahn, P. E.; M, *J. Phys. Chem. B.* **2003**, *107*, 3944.
(36) Hattori, T.; Toriashi, T.; Tsuneda, T.; Nagasaki, S.; Tanaka, S. *J. Phys. Chem. A* **2005**, *109*, 10403.
(37) Rickard, G. A.; Gomez-Balderas, R.; Brunelle, P.; Raffa, D. F.; Rauk, A. *J. Phys. Chem. A* **2005**, *109*, 8361.
(38) Marino, T.; Toscano, M.; Russo, N.; Grand, A. *J. Phys. Chem. B* **2006**, *110*, 24666.
(39) Rimola, A.; Rodríguez-Santiago, L.; Sodupe, M. *J. Phys. Chem. B* **2007**, *111*, 5740.
(40) Powell, K. J.; Brown, P. L.; Byrne, R. H.; Gajda, T.; Hefter, G.; Sjöberg, S.; Wanner, H. *Pure Appl. Chem.* **2007**, *79*, 895.
(41) Duncombe, B. J.; Duale, K.; Buchanan-Smith, A.; Stace, A. J. *J. Phys. Chem. A* **2007**, *111*, 5158.
(42) O'Brien, J. T.; Williams, E. R. *J. Phys. Chem. A* **2008**, *112*, 5893.
(43) Li, J.; Fisher, C. L.; Chen, J. L.; Bashford, D.; Noodleman, L. *Inorg. Chem.* **1996**, *35*, 4694.
(44) Martin, R. L.; Hay, J. P.; Pratt, L. R. *J. Phys. Chem. A* **1998**, *102*, 3565.
(45) Tsushima, S.; Wahlgren, U.; Grenthe, I. *J. Phys. Chem. A* **2006**, *110*, 9175.
(46) de Abreu, H. A.; Guimarães, L.; Duarte, H. A. *J. Phys. Chem. A* **2006**, *110*, 7713.
(47) Guimarães, L.; de Abreu, H. A.; Duarte, H. A. *Chem. Phys.* **2007**, *333*, 10.
(48) de Noronha, A. L. O.; Guimarães, L.; Duarte, H. A. *J. Chem. Theory Comput.* **2007**, *3*, 930.
(49) Kubicki, J. D. *J. Phys. Chem. A* **2001**, *105*, 8756.
(50) Vallet, V.; Wahlgren, U.; Grenthe, I. *J. Am. Chem. Soc.* **2004**, *126*, 12786.
(51) Uudsemaa, M.; Tamm, T. *J. Phys. Chem. A* **2003**, *107*, 9997.
(52) Blumberger, J.; Bernasconi, L.; Tavernelli, I.; Vuilleumier, R.; Sprik, M. *J. Am. Chem. Soc.* **2004**, *126*, 3928.
(53) Blumberger, J.; Sprik, M. *Theor. Chem. Acc.* **2006**, *115*, 113.

(54) Hush, N. S.; Schamberger, J.; Bacskay, G. B. *Coord. Chem. Rev.* **2005**, *249*, 299.
(55) Jaque, P.; Marenich, A. V.; Cramer, C. J.; Truhlar, D. G. *J. Phys. Chem. C* **2007**, *111*, 5783.
(56) Klamt, A.; Schüürmann, G. *J. Chem. Soc., Perkin Trans. 2* **1993**, 799.
(57) Ahlrichs, R.; Bär, M.; Häser, M.; Horn, H.; Kölmel, C. *Chem. Phys. Lett.* **1989**, *162*, 165.
(58) Becke, A. D. *Phys. Rev. A* **1988**, *38*, 3098.
(59) Lee, C. T.; Yang, W. T.; Parr, R. G. *Phys. Rev. B* **1988**, *37*, 785.
(60) Peschke, M.; Blades, A. T.; Kebarle, P. *J. Am. Chem. Soc.* **2000**, *122*, 10440.
(61) Tunell, I.; Lim, C. *Inorg. Chem.* **2006**, *45*, 4811.
(62) Carl, D. R.; Moision, R. M.; Armentrout, P. B. *Int. J. Mass Spectrom.* **2007**, *265*, 308.
(63) Bryantsev, V. S.; Diallo, M. S.; van Duin, A. C. T.; Goddard, W. A., III. *J. Chem. Theory Comput* **2009**, *5*, 1016.
(64) Hay, P. J.; Wadt, W. R. *J. Chem. Phys.* **1985**, *82*, 299.
(65) *Jaguar, version 7.0, User Manual*; Schrödinger, LLC: New York.
(66) Pavelka, M.; Burda, J. V. *Chem. Phys.* **2005**, *312*, 193.
(67) Perdew, J. P.; Burke, K.; Emzerhof, M. *Phys. Rev. Lett.* **1996**, *77*, 3865.
(68) Perdew, J. P. *Phys. Rev. B* **1986**, *33*, 8822.
(69) *Jaguar, version 7.5*, Schrödinger, LLC: New York, 2008.
(70) Klamt, A.; Jonas, V.; Bürger, T.; Lohrenz, C. W. *J. Phys. Chem. A* **1998**, *102*, 5074.
(71) Bondi, A. *J. Chem. Phys.* **1964**, *64*, 441.
(72) Tannor, D. J.; Marten, B.; Murphy, R.; Friesner, R. A.; Sitkoff, D.; Nicholls, A.; Ringnalda, M.; Goddard III, W. A.; Honig, B. *J. Am. Chem. Soc.* **1994**, *116*, 11875.
(73) Bryantsev, V. S.; Diallo, M. S.; Goddard, W. A., III. *J. Phys. Chem. B* **2008**, *112*, 9709.
(74) Marenich, A. V.; Olson, R. M.; Chamberlin, A. C.; Cramer, C. J.; Truhlar, D. G. *J. Chem. Theory Comput.* **2007**, *3*, 2055.
(75) Gutowski, K. E.; Dixon, D. A. *J. Phys. Chem. A* **2006**, *110*, 8840.
(76) Siboulet, B.; Marsden, C. J.; Vitorge, P. *Chem. Phys.* **2006**, *326*, 289.
(77) Kamerlin, S. C. L.; Haranczyk, M.; Warshel, A. *J. Phys. Chem. B* **2009**, *113*, 1253.
(78) Pliego, J. R., Jr.; Riveros, J. M. *J. Phys. Chem. A* **2001**, *105*, 7241.
(79) Bock, C. W.; Markham, G. D.; Katz, A. K.; Glusker, J. P. *Theor. Chem. Acc.* **2006**, *115*, 100.
(80) Asthagiri, D.; Pratt, L. R.; Ashbaugh, H. S. *J. Chem. Phys.* **2003**, *119*, 2702.
(81) Ilcheva, L.; Bjerrum, J. *Acta Chem. Scand. A* **1976**, *30*, 343.
(82) Kelly, C. P.; Cramer, C. J.; Truhlar, D. G. *J. Phys. Chem. B* **2006**, *110*, 16066.
(83) Camaioni, D. M.; Schwerdtfeger, C. A. *J. Phys. Chem. A* **2005**, *109*, 10795.
(84) Tissandier, M. D.; Cowen, K. A.; Feng, W. Y.; Gundlach, E.; Cohen, M. H.; Earhart, A. D.; Coe, J. V. *J. Phys. Chem. A* **1998**, *102*, 7787.
(85) Warshel, A.; Levitt, M. *J. Mol. Biol.* **1976**, *103*, 227.
(86) Car, R.; Parinello, M. *Phys. Rev. Lett.* **1985**, *55*, 2471.
(87) Svozil, D.; Jungwirth, P. *J. Phys. Chem. A* **2006**, *110*, 9194.
(88) Miller, D. J.; Lisy, J. M. *J. Chem. Phys.* **2006**, *124*, 024319.
(89) Bush, M. F.; Saykally, R. J.; Williams, E. R. *J. Am. Chem. Soc.* **2008**, *130*, 15482.
(90) Lee, H. M.; Tarkeshwar, P.; Kim, K. S. *J. Chem. Phys.* **2006**, *121*, 4657.
(91) Varma, S.; Rempe, S. B. *Biophys. Chem.* **2006**, *124*, 192.

JP904816D